ACS OMEGA

http://pubs.acs.org/journal/acsodf

Article

Evaluation of the Dielectric and Insulating Properties of Newly Synthesized Ethylene/1-Hexene/4-Vinylcyclohexene Terpolymers

Amjad Ali, Khulood Fahad Saud Alabbosh, Ahmad Naveed,* Azim Uddin, Yanlin Chen, Tariq Aziz, Jamile Mohammadi Moradian, Muhammad Imran, Lu Yin, Mobashar Hassan, Waqar Ahamad Qureshi, Muhammad Wajid Ullah, Zhiqiang Fan, and Li Guo*

Cite This: *ACS Omega* 2022, 7, 31509−31519

Read Online

ACCESS | Metrics & More | Article Recommendations

ABSTRACT: Terpolymerizations of newly synthesized ethylene (E), vinylcyclohexene (VCH), and 1-hexene were carried out with symmetrical metallocene catalysts *rac*-Me_2Si(2-Me-4-Ph-Ind)$_2ZrCl_2$ (catalyst A) and *rac*-Et(Ind)$_2ZrCl_2$ (catalyst B). X-ray diffractometry (XRD), scanning electron microscopy (SEM), differential scanning calorimetry (DSC), high-temperature gel permeation chromatography (GPC), and nuclear magnetic resonance (NMR) spectroscopy were used to evaluate the behavior and microstructure of the polymers. The activity of catalyst B was 1.49×10^6 gm/mmol$_{Mt}$·h), with a T_m of 73.45 (°C) and ΔH_m of 43.19 (J/g), while catalyst A produced first higher 1-hexene, 19.6 mol %, and VCH contents with a narrow molecular weight distribution (MWD). In previous reports, ethylene propylene monomer dienes (EPDM) had a low content and were used for dielectric and insulating properties with nanomaterials. Second, this paper presents a kind of elastomeric polymers based on E/1-hexene and VCH with a high dielectric constant (k = 6−4) and mechanical properties. In addition, low dielectric loss suggests the suitable application potential of these polymeric materials for the fabrications of capacitors. Also, this work reveals that these polymers can be a better candidate for high-voltage electrical insulation due to their enhanced dielectric, mechanical, and thermal characteristics. To examine the insulating property, the interface characteristics of the polymer were evaluated using electrochemical impedance spectroscopy (EIS) with a frequency range of 1×10^5−0.01 Hz and an amplitude of 5.0 mV. EIS is an effective method to investigate the polymers' interfacial electron transfer characteristics. The EIS Nyquist plot showed high Warburg impedance features in the low-frequency domain with straight lines without a semicircle, suggesting that the property of the polymer owing to the high electrical resistance and poor conductivity for ionic kinetics in the electrolyte may have surpassed that of the semicircle. Although the slope of low frequencies in polymers holding potent exoelectrogenic bacteria (*Shewanella oneidensis* MR-1) as a charge carrier in the electrolyte could significantly reduce the Warburg resistance, it still could not improve the conductivity, which demonstrated that the external charge supply could not alter the insulating property in the used polymers.

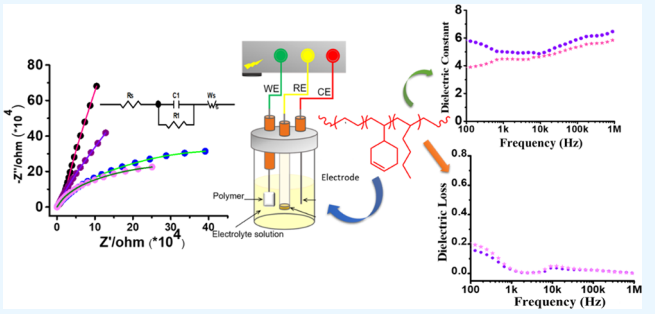

1. INTRODUCTION

Ethylene propylene diene monomer (EPDM) polymeric materials play an important role in daily life and significantly contribute to mechanical and electrical manufacturing. In contrast to inorganic materials such as mica, ceramics, and glasses, polymeric materials have significant advantages, including easy processing, better fabrication, low dielectric losses, and excellent insulating properties. Furthermore, EPDM-based polymeric materials are also used as the reinforcing structural element for electric products.[1]

Ethylene propylene with dienes and EPDM elastomers are manufactured on a large scale, with annual production exceeding 100 million tons.[2−5] These elastomers were produced with heterogeneous Ziegler−Natta (Z-N) catalysts through ion coordination-based polymer reactions. The Ziegler−Natta catalyst system was developed in the 1960s and has been broadly used up to now in polyolefin industries. From the discovery of the Ziegler−Natta catalyst to 1990, the manufacturing of E.P. and EPDM was largely based on vanadium-based catalysts such as $VOCl_3$ and VCl_4. The disadvantages of these catalysts were low stability and catalytic activity. In addition, with a large amount of vanadium (V) in the polymeric product, very expensive equipment have to be used to

Received: July 5, 2022
Accepted: August 16, 2022
Published: August 25, 2022

remove the residual V. To overcome these problems, academic and industrial researchers used single-site homogeneous metallocene catalysts for the synthesis of E and P homopolymers, E.P., and EPDM since the 1990s. Numerous metallocene catalysts with different substituents have been investigated to manufacture these polymers.

The development of novel catalysts based on group 4 metals has re-examined polyolefin chemistry over the past 30 years due to the fast expansion of technology and materials. The higher activity, better selectivity, control of molecular weight, and a wide range of α-olefins ranging from plastomers to elastomers are all advantages of metallocene catalysts. In addition, many variables influence the elastomeric characteristics of a polymer, including the amount of co- or termonomers present in the polymer, its molecular weight (M_w), and molecular weight distribution (MWD) metallocene catalysts can control.[2,6−9] Due to these advantages of metallocene, it was estimated in the year 2006 that about more than 60 million tons of polyolefin were manufactured, which makes up about 50% of regular-use plastics.[2−5] It means that other daily-use plastics can be replaced with EPDM and other types of polyolefin, such as E with 1-hexene and E/I-hexene/dienes in the future. What is the main reason for this? Its impact on daily life has considerable applications, ranging from simple plastic bags to highly sophisticated capacitors and module fibers.[10−12] Additionally, they are employed as a structural element for electrical devices, strengthening the structure.[1,13−16] Furthermore, olefins are an elastomeric material with outstanding electrical characteristics when adequately formulated, including heat and ozone resistance, an extensive range of hardness and stress resistance, and better chemical resistance, particularly to polar media.[17−19] Their electrical solid insulation qualities make them suitable for use in low- to moderate-voltage wires and cables (up to 35 kV). Measuring and analyzing the dielectric characteristics are a quantitative approach used to understand the charge transfer mechanisms in the polymer.[20−22] These properties provide a different approach for discovering innovative uses for these new polymeric materials. Charge transport capabilities in polymeric materials have been the subject of several studies and theoretical models. Polymeric materials have charge carriers that are localized, which hence move in the material between the localized states either by hopping or tunneling through the potential barriers.[23−25]

In this study, we use a single-site bridged metallocene catalyst for the new kind of E/1H/VCH terpolymers with a higher content of VCH, further chosen as the insulating matrix materials because of their outstanding electrical and mechanical resistance properties and suitable for potential use in electrical wires and cables. They are excellent isolators because they are nonpolar polymers resistant to alkalies and acids.[26] Furthermore, frequency-dependent conducting mechanisms in new materials are an essential aspect to explore. The synthesis and dielectric properties of E/1-H/VCH terpolymers are thoroughly reported in this article. However, the synthesis of these new elastomers to prepare dielectric elastomers has been unreported to date. Therefore, this paper delineates a synthesis of E/1-H/VCH terpolymers catalyzed with catalyst A and catalyst B to prepare dielectric materials with enhanced dielectric properties. These metallocene catalysts allow the possibility to tailor the polyolefin structure in a new way that has not been reported before.

2. METHODS

2.1. Materials. The asymmetric metallocene polymerization catalysts *rac*-$Me_2Si(2\text{-Me-4-Ph-Ind})_2ZrCl_2$ catalyst A (Shanghai Research Institute of Chemical Industry, Shanghai, China), *rac*-$Et(Ind)_2ZrCl_2$ catalyst B (Sigma-Aldrich), and the borate $[Ph_3C][B(C_6F_5)_4]$ cocatalyst were donated by Sinochem Lantain, Zhejiang Research Institute of Chemical Industry Co., Ltd. Hangzhou, PR. China. Borate and both catalysts were diluted in toluene, while triisobutylaluminium (TIBA) (Albemarle Co) was diluted in *n*-heptane and held under nitrogen. Ethylene with 99.9% purity (Zhejiang Gas mixing Co. Hangzhou, China.) was used. 1-Hexane and VCH were bought from Arcos Organics Chemicals China and purified through dehydration using 4 Å molecular sieves and collected using the vacuum distillation process.

2.2. Polymerization. The E/1-H/VCH terpolymerization reactions were carried out in a 100 mL Schlenk round-bottom glass reactor. A pure form of E was added to the polymerization reactor, followed by injections of 1-hexene and VCH. TIBA was then added and allowed to run for 5 min before being followed by a metallocene and borate activator to initiate polymerization. After the planned time, the reaction was quenched with dehydrated ethanol containing 2 percent HCl, which decomposed the TIBA, borate, and metallocene and allowed the polymerization to stop. Before drying under vacuum, the terpolymers were precipitated in ethanol and subjected to an intensive purification technique that included many steps.[27,28]

2.3. Characterization. The NMR spectra were measured using a Varian Mercury plus 300 spectrometers (Varian Corporation) (75 MHz). Dichlorobenzene-d4 was used as the test solvent, and it had a concentration of 10% by weight in the sample. A temperature of 120 °C was employed to obtain NMR spectra, with hexamethyldisiloxane serving as an internal chemical shift standard.[15]

2.4. Gel Permeation Chromatography (GPC). To measure the M_w and MWD, we use PL-gel MIXED-B columns and 1,2,4-trichlorobenzene as the eluent at a flow rate of 1.0 mL/min at a temperature of 150 °C, universal calibration against thin polystyrene standards was performed, and the results were successful for both M_w and MWD.[13]

2.5. Differential Scanning Calorimetry (DSC). A TA Q200 instrument was used to examine the thermal behavior of terpolymers, and it was calibrated with indium and water before being utilized. Initially, the sample was heated to 150 °C for 5 min and then cooled to 20 °C at a rate of 10 °C/min. To eliminate thermal history, the melting curve was finally recorded by heating the sample to 180 °C at a rate of 10 °C/min.[29,30]

2.6. Scanning Electron Microscopy (SEM). Using a Hitachi S-4800 system coupled to an energy-dispersive X-ray spectroscopy (EDS) system, the morphology of the samples was investigated using scanning electron microscopy (SEM).[27]

2.7. X-ray Diffractometery (XRD). The crystal structure of the E/1H/VCH terpolymers and insertion of VCH were also analyzed with an X-ray diffractometer (XRD) from the Zhejiang university chemical engineering department.

2.8. Flexural Properties of the E/1H/VCH Terpolymer. *2.8.1. E/1-Hexene/VCH Terpolymer Tensile Specimen.* The tensile behavior of the newly synthesized E/1-H/VCH terpolymer samples was investigated using an Instron universal tensile machine. Table 1 shows the information about the specimen.

https://doi.org/10.1021/acsomega.2c04123
ACS Omega 2022, 7, 31509−31519

Table 1. Specimen Details

s.no.	description	value (mm)
1	width of graph	25
2	width of graph	5
3	inner radius	25
4	radius for center shape	11
5	length for grip	15
6	gauge length	20
7	total length	50
8	thickness	0.2

The polymer samples were prepared at 80 °C for 5 min using the compression−molding technique; the design of the sample and machine is shown in Figure 1.

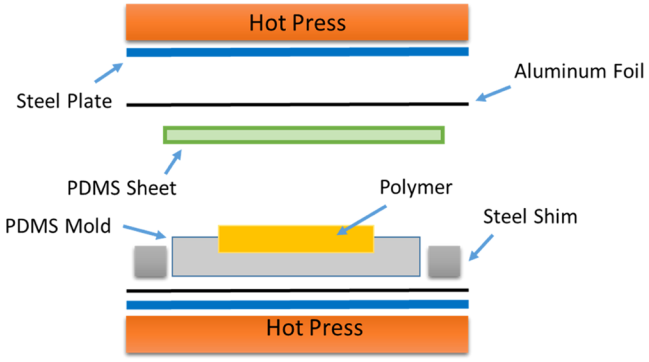

Figure 1. Compression−molding technique.

A dielectric material test fixture measured the capacitance on an LCR meter (TH2826A). The electrode diameter of the sample was 10mm, and the thickness was about 2 mm. The scanning frequency was from 100 Hz to 1 MHz at room temperature. The relative permittivity of the materials was calculated by eq 1

$$\varepsilon = \frac{C_z}{\varepsilon_0 A} \quad (1)$$

There are four variables in this equation: C (capacitance measurement), z (elastomer thickness), 0 (vacuum permeability), and A (effective area)

2.9. Electrochemical Impedance Spectroscopy (EIS). To examine the insulating property of E/1H/VCH terpolymers, the interface characteristics of the polymer material were evaluated using electrochemical impedance spectroscopy (EIS) with a frequency range of 1×10^5−0.01 Hz and an amplitude of 5.0 mV. The ethylene and diene-based polymer material analyses were performed using the CHI electrochemical workstation (CHI660E, Cheng Hua Instrument Co. Ltd., Shanghai) with a three-electrode system. To operate the system, the polymers served as the working electrode, with platinum (Pt) wire as the counter electrode and an external electrode, saturated calomel, as a reference electrode (SCE, 0.241 V vs SHE).[31]

Furthermore, to test the EIS property of the polymers under mild conditions, the experimental state was characterized at room temperature with two sets of operating conditions using phosphate-buffered saline (PBS, pH 7.2) as an electrolyte without charge carriers and with a negative charge carrier using a potent exoelectrogenic bacterial cell of *Shewanella oneidensis* MR-1. *S. oneidensis* MR-1, a model strain of exoelectrogenic bacteria (EEB), can utilize a wide range of extracellular electron acceptors (e.g., iron, manganese oxides, oxygen, and sulfur species) in its cellular metabolism and growth for anaerobic electrode respiration and thus play important roles in environmental bioremediation, energy production from wastes, and biogeochemical cycling of metals in environments.[32] Similarly, to measure the ohmic resistance (R) values of polymers (catalyst A and catalyst B), the potential differences between two points in voltage (V) proportional to the current (I) were calculated through Ohm's law ($R = V/I$).[33]

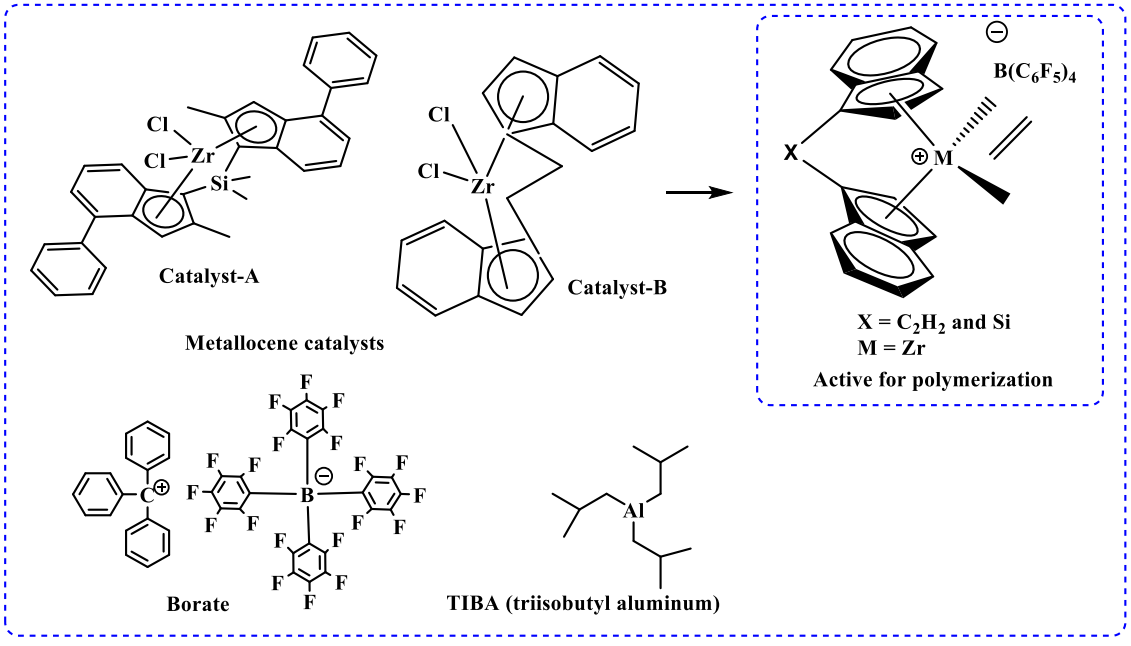

Figure 2. Structure of the metallocene catalysts and active species for polymerization.

https://doi.org/10.1021/acsomega.2c04123
ACS Omega 2022, 7, 31509−31519

Scheme 1. Synthesis of E/1-H/VCH Terpolymers with Symmetrical Metallocene

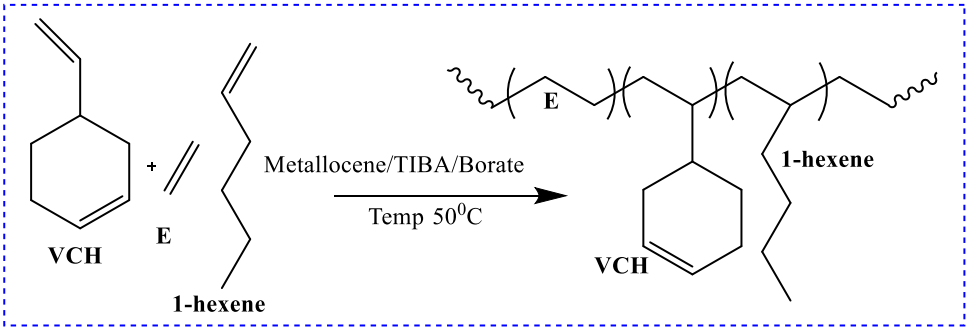

Table 2. Ethylene/1-Hexene/VCH Terpolymerization Catalyzed by Symmetrical Metallocene[abe]

run	cat	yield (g)	activity (10^6 gm/mmol$_{Mt}$·h)	M_w (kg/mol)	$Đ$	T_m (°C)	ΔH_m (J/g)
1	catalyst A	0.61	1.48	59.00	2.22	123.1	0.3
2	catalyst B	1.49	3.6	56.30	2.66	92.6	58.8

[a]Reaction conditions: Catalyst 1.25 μmol, borate 2.5 μmol, TIBA 1000 μmol, 1-hexene 0.12 mol/L, VCH 0.06 mol/L, ethylene pressure = 0.1 MPa, temperature = 50 °C, and solvent: toluene (50 mL). [b]Determined by GPC. [e]Determined by DSC.

3. RESULTS AND DISCUSSION

Before analyzing the dielectric properties, we first synthesized E/1-H/VCH terpolymers with different mole ratios of 1-hexene and VCH using two symmetrical metallocene-catalyzed polymerization techniques in a nonpolar solvent; the structure of the asymmetric metallocenes is shown in Figure 2. Both catalysts showed C_2 symmetry but different ligand structures, which means that they produce E/1-hexene/VCH terpolymers with various activities and different monomer compositions, depending on the electronic impact and size of ligands attached to the Zr metal. According to the literature, catalyst B is one of the simplest C_2-symmetric polymeric catalysts systematically studied and well known to produce polymers with a high polymerization and diene content.

One of the most popular industrial methods is the slow coordination polymerization method to produce polymers with <5% dienes. To increase the insertion of termonomers (diene) in E-1-hexene, we chose VCH with a less steric effect than other cyclic dienes (NB, VNB, ENB, etc.), which permitted us to insert it in the polymer chain through the exocyclic bond; see Scheme 1.

To increase the insertion of the exocyclic π bond of VCH and the 1-hexene π bond silly bridge and ethylene bridge catalyst system was the best choice.

Our previous study on E/P/dienes (80/20/0.06 and 80/20/0.12 mole ratios) catalyzed with metallocene/TIBA/borate and that of Jongsomjit et al. on E/P/dienes (50/50/0.06 mole ratios) found that enhancing VCH concentrations over 0.06 mol/L lowered the catalytic activity considerably.[13,34] Similarly, a higher amount of cyclic nonconjugated diene addition could result in a declined activity of metallocene polymerization as investigated by Malmberg and Löfgren et al., although it should be noted that large amounts of (~2−5 mol %) of dienes (VCH) were technically required to produce the dielectric properties of the polymers.[35−38] Following on that study, at first, E/1-H/VCH terpolymerization was run at a constant E/1-hexene/VCH feed ratio of 0.12/0.06. The amount of 0.06 mol/ L VCH was enough to maintain the higher activities of both catalysts because of the low steric flexibility of the double bond in the cyclohexene ring.[13] As shown in Table 2, catalyst B showed higher activity than catalyst A and so did the formerly produced terpolymer with a lower VCH content than that with catalyst A. According to Fan et al., the copolymerization of E/P (50/50) with the addition of VCH caused evident activity enhancement.[34] In contrast with the catalyst A-catalyzed E/P/diene terpolymers, more negative effects of diene addition were reported in the literature.[27,39] In addition, compared to propylene, a higher content of 1-hexene in the feed caused a more substantial activation effect. According to Mortazavi, among the E/P/diene terpolymers, reducing the ethylene content of the monomer feed caused a more significant deactivation effect by the diene.[27,40] It is interesting to compare the activities; for E/P/VCH with catalyst B/methylaluminoxane (MAO) and catalyst B /TIBA/borate, the activities were about 2.8×10^6 and 3.14×10^6 gm$_{polym}$/mol$_{Mt}$*h, which are relatively lower than the activity of E/1-H/VCH terpolymers catalyzed with catalyst B/borate/TIBA under similar conditions.[13,15] It means that 1-hexene is an effective comonomer for synthesizing elastomers with higher activity. However, the increased activities were more pronounced with VCH in both cases.[13,14,34] The comonomer effect can explain increases in the polymerization activity. Guo et al. claimed that the copolymerization activity of E/P was greater than their homopolymerization activity.[13] They observed that the faster insertion of ethylene molecules could not explain the increased rate but was likely the result of activating dormant catalyst sites by ethylene.[14] Some other characteristic explanations have also been reported in the literature to describe this phenomenon, including the improved diffusion rates and preventing the solubilization of active sites of a catalyst by incorporating co- or termonomers and trigger mechanisms.[8,27] However, based on this explanation, addition of 1-hexene would improve the attachment of ethylene monomers to the catalyst's active sites, resulting in increased activity. In contrast, propylene inhibits the attachment of ethylene to the catalyst's active sites through the solubilization of active sites.[14,41]

3.1. Thermal Properties. The thermal properties (T_m and ΔH_m) of E/1-hexene/VCH were obtained from DSC and are listed in Table 2. According to the ^{1}H NMR results, the content of 1-hexene and VCH is more in the catalyst A-catalyzed polymer, leading to reduced crystallinity properties. The T_m of catalyst A-catalyzed E/1-hexene/VCH elastomers is 123.1 (°C),

https://doi.org/10.1021/acsomega.2c04123
ACS Omega 2022, 7, 31509−31519

which is higher than that of catalyst B-catalyzed polymers. In contrast, catalyst B-catalyzed E/1-hexene/VCH terpolymers with a higher content of E become crystalline materials; see Figure 3. Similar results were reported by Phoowakeereewiwat et al. work where the content of E increased in the terpolymerization of E/P/diene catalyzed with catalyst B/MMAO.[13,34] In conclusion, the thermal properties are firmly dependent on the mole percent of VCH and 1-hexene. It is required to determine the incorporation of VCH in the polymer chain, which is explained in the next part of this paper.

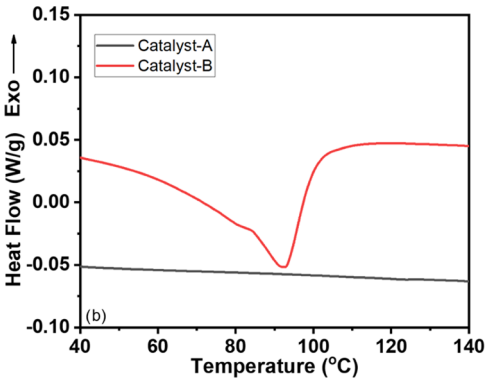

Figure 3. Thermal properties of E/1H/VCH terpolymerization with catalyst A and catalyst B under similar conditions.

The morphological investigations of the synthesized polymers were done through scanning electron microscopy analysis (SEM), as displayed in Figure 4a–f. The catalyst A-catalyzed polymer SEM images exhibited highly dense and interlinked thick polymeric structures with little porosity. The more elastomeric-like nature of the polymer is reflected in the corresponding SEM micrographs. (Figure 4a–c). Multiple small islands like bumpy surfaces revealed the compactness and homogeneity of the surface. However, the catalyst B-catalyzed polymer revealed a typical flatter surface morphology that comprises thin polymeric strings interconnected throughout the network, as seen in Figure 4d–f. The high-resolution SEM micrographs further clarify polymeric strings' networking and homogenous surface covering. From the SEM analysis, it was found that both the polymers offered homogeneous and clear surface morphology.

3.2. NMR. It is well known that NMR spectroscopy is one of the sanative and powerful techniques to identify the polymer microstructure and co- or termonomer mole %. It is required to determine the incorporation of VCH in the polymer chain through exocyclic π bonds or endocyclic π-bonds. The characteristic ^{1}H NMR spectra for E/1-hexene/VCH with both metallocene catalysts are illustrated in Figure 5. It can be observed that the ^{1}H NMR spectra for E/1-hexene/VCH have peaks in the region of 5.4–5.6 ppm for VCH and 1.5–0.5 ppm for E and 1-hexene, which clearly show the insertion of VCH exocyclic π bonds. In addition, these peaks indicate that more than enough amount of 1-hexene and VCH is incorporated into the polymer chain under the specified conditions; see Table 3. In our previous study, we observed more than 0.06 mol/L VCH during the insertion of a propylene comonomer. Jongsomjit and his group described comparable results in the copolymerization

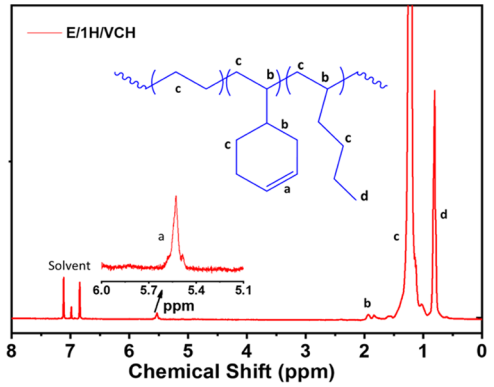

Figure 5. ^{1}H NMR spectra of the E/1-H/VCH terpolymer catalyzed by the metallocene/borate/TIBA catalyst system.

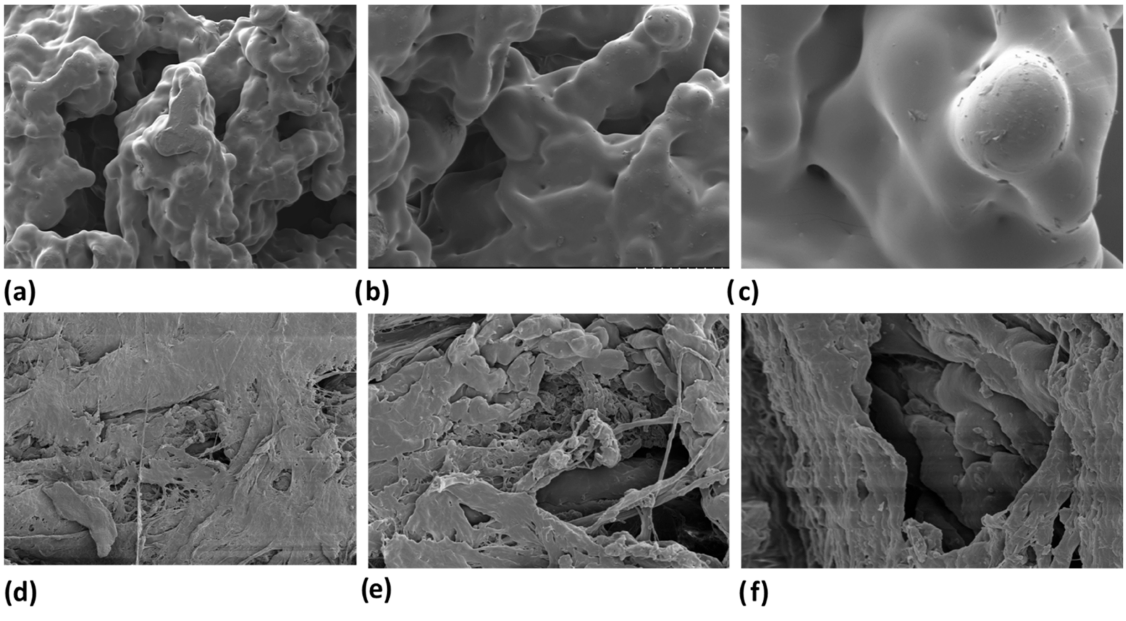

Figure 4. SEM images of E/1H/VCH terpolymers with catalyzed A (a–c) and E/1H/VCH terpolymers with catalyze B (d–f).

https://doi.org/10.1021/acsomega.2c04123
ACS Omega 2022, 7, 31509–31519

Table 3. Monomers Composition in Ethylene/1-Hexene/VCH Terpolymerization Calculated by H NMR Spectroscopy[a]

run	cat	ethylene (mol %)	1-hexene (mol %)	VCH (mol %)
1	catalyst A	79.3	19.9	0.77
2	catalyst B	93.8	6.0	0.16

[a]Conditions: Solvent = dichlorobenzene-d_4, sample concentration 10% by weight, temperature of 120 °C, number of scans 400, and hexamethyldisiloxane serving as an internal chemical shift standard.

of ethylene with higher α-olefins such as 1-octene and 1-decene.[34]

In addition, the XRD pattern of E/1H/VCH is shown in Figure 6, and the characteristic peaks of E/1H/VCH

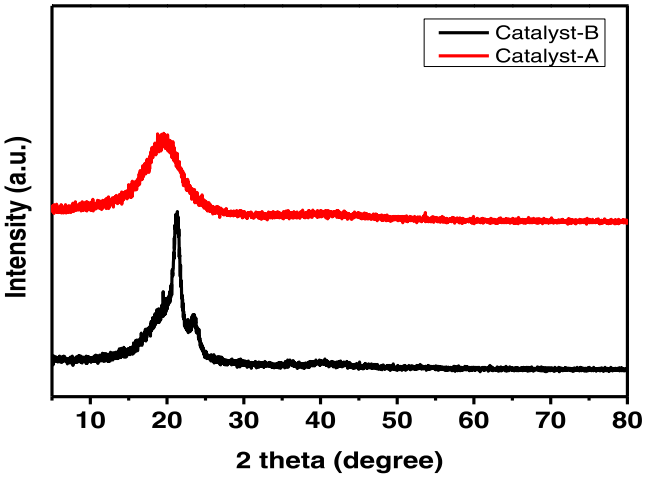

Figure 6. XRD pattern of E/1H/VCH terpolymers produced with catalyst A and catalyst B.

terpolymers produced with catalyst A and catalyst B can be observed, where the red peak shows catalyst A and blue peak shows catalyst B, compared with E/P/diene terpolymers,[42] which give evidence of VCH insertion same as in EPDM.

3.3. Molecular Weight (MW). Based on our investigation data, the effect of catalyst ligands and bridging atoms inserted between the metal and ligands of the catalysts could be drawn from the resulting E/1-hexene/VCH terpolymer activities, VCH incorporation, thermal properties, molecular weight, and molecular weight distribution. The addition of VCH/1-hexene (0.06/0.12 mol/L) could modify the behaviors of E/1-hexene/VCH terpolymers using an asymmetrical zirconocene/borate/TIBA catalyst system. The M_w of E/1-hexene/VCH is higher than that of E/P/VCH terpolymers. Generally, sufficient higher M_w is required for outstanding tensile properties of the EPDM that work as an elastomer. As seen in Table 1, the E/1-hexene/VCH terpolymers produced with catalyst A have higher M_w than with catalyst B. However, in our previous study, catalyst B/TIBA/Borate showed a higher (51.0 kg/mol) M_w when VCH was inserted as a termonomer in the E/P copolymer.[8,27] The polydispersity index ($Đ$) of the E/1-hexene/VCH terpolymers produced with both catalysts is narrow (see Figure 7). Its value was still obvious and larger than 2, which is closer to the true single-site metallocene catalyst, suggesting the existence of several active sites in the catalytic system involved in inserting E, 1-hexene, and VCH in the polymer backbone.

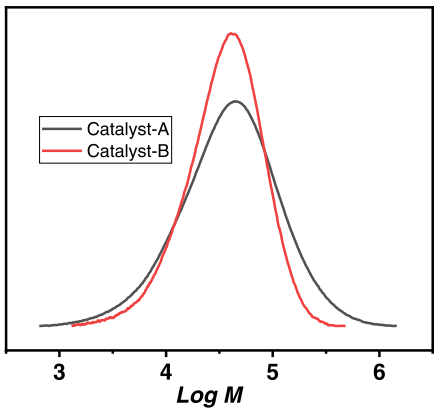

Figure 7. Molecular weight distribution of E/1H/VCH polymers under the same polymerization conditions.

3.4. Dielectric Properties of the E/1-Hexene/VCH Terpolymer. The silicone rubber and EPDM polymeric material are generally used for reinforced insulation due to their excellent insulation performance. Following this study, we chose E/1-H/VCH terpolymers as dielectric materials because they exhibit a higher amount of 1-hexene and VCH. First, we calculate the dielectric properties of catalyst A-catalyzed E/1-H/VCH terpolymers at room temperature and then for catalyst B-catalyzed polymer. The dielectric constant and dielectric loss variation were investigated by varying the applied field's frequency. As shown in Figure 8, the sample shows high

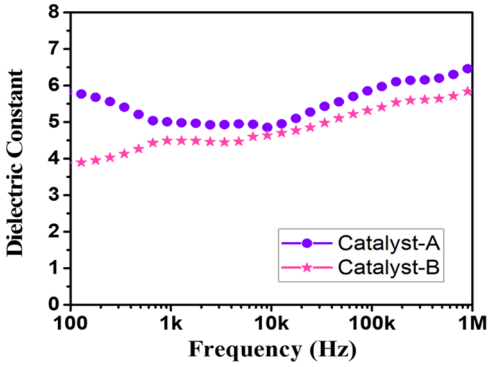

Figure 8. Frequency dependence of the dielectric constant of the catalyst A- and catalyst B-catalyzed E/1-H/VCH terpolymer samples in the frequency range of 100 Hz−1 MHz.

dielectric constant values of around 6 and 4 at a lower frequency. However, with a further increase in the frequency from 1 Hz to 1 MHz in the applied field, the dielectric constant values were slightly increased. For example, the dielectric constant was reduced from 6.00 to 4.65 for catalyst A-catalyzed E/1-H/VCH terpolymers within the frequency range from 100 to 1 kHz. In contrast, catalyst B-catalyzed E/1H/VCH terpolymers demonstrated comparatively lower dielectric constants, varying from 4.00 to 4.50 under the same frequency level. However, as the frequency was increased from 100 Hz to 1 kHz, the dielectric constant of catalyst B-catalyzed polymers increased. In addition, as the applied field frequency was increased, both catalysts exhibited comparable dielectric constants. According to Kan Zhang, the dielectric constant of the polybenzoxazines was decreased when the frequency of the applied field was increased to 100 Hz; catalyst A-catalyzed E/1-H/VCH terpolymers showed similar behavior at a low-frequency level.[43] In general,

https://doi.org/10.1021/acsomega.2c04123
ACS Omega 2022, 7, 31509−31519

at 1 MHz, the dielectric constants of conventional EPDM and benzoxazine are typically in the range of 3−4.[44] As expected, newly synthesized E/1-H/VCH terpolymers with moderate mol % of VCH catalyzed by the symmetrical metallocene catalyst system exhibited a high dielectric constant, which is higher than that previously reported in the literature with norbornene-functionalized benzoxazine. Notably, the higher dielectric constants of the E/1-H/VCH terpolymers are comparable to those of ethylene/propylene/diene (EPDM)/NB nanocomposites.[20] Therefore, the introduction of VCH and 1-hexene with ethylene instead of propylene increased the dielectric constant significantly, and 1-hexene importantly increased the incorporation rate of VCH as compared to P. In the terpolymer chain, the network formed by connection of the exocyclic π-bonds of VCH and π-bonds of 1-hexene might have a higher dielectric constant.

The change in dielectric loss with increasing frequency is because of the displacement of electric charges inside the polymer. The variation of dielectric loss was calculated at different frequencies[20] for both metallocene-catalyzed terpolymers, as shown in Figure 9.

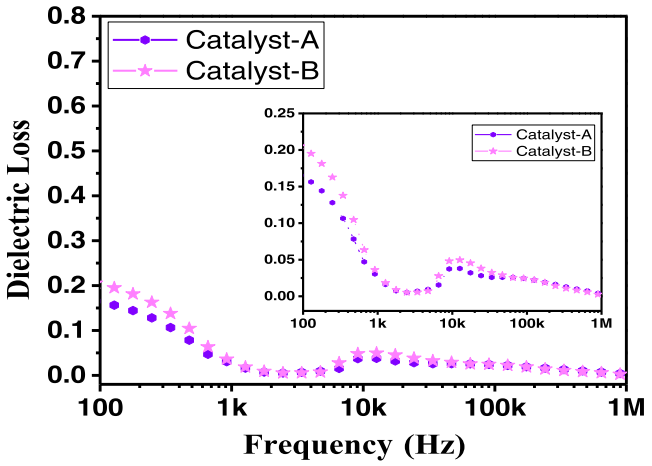

Figure 9. Frequency dependence of dielectric loss of the catalyst A- and catalyst B-catalyzed E/1-H/VCH terpolymer samples in the frequency range of 100 Hz−1 MHz.

The graph shows that the samples show a low dielectric loss, values of around 0.2 and 0.16, at a lower frequency of 100−1 kHz. We observed that the dielectric loss shows good consistency with increased frequency. A high dielectric constant and low loss have always been contradictory points, and the loss of high-dielectric materials is generally higher. Dielectric loss for both samples shows a low-value plateau-like polymer material at higher frequencies. At low frequencies, the dielectric loss values were found to decrease. The dielectric loss is characterized by relaxation frequency for both samples. The change in dielectric loss with increasing frequency is because of the displacement of electric charges inside the polymer[24] and due to high resistivity caused by grain boundaries. Moreover, the catalyst A-catalyzed sample shows less dielectric losses than the catalyst B-catalyzed sample, suggesting the suitable application of the polymeric material in the fabrications of capacitors.[45] The results again demonstrate that the electromechanical properties and performance of dipole elastomers are affected by the combined influence of the structure and the content of the dipoles.

EIS is a powerful technique, which was used to examine the properties of interfacial electron transfer processes in polymers. The obtained data by EIS are fitted with a simple electrical equivalent circuit model using ZView software integrated with SAI measurement software (R_S (C(R_{CT}.W_S))) (Figure 10a). The fitting data could estimate the values of individual resistances (i.e., ohmic resistance, Warburg resistance, etc.) in this study. The E/1-hexene/VCH terpolymers were used as the working electrode, with platinum (Pt) wire as the counter electrode and an external electrode, saturated calomel, as a reference electrode (SCE, 0.241 V vs SHE).[31] The three-electrode system is depicted schematically in Scheme 2.

As shown in Figure 10a, all EIS Nyquist plots exhibited high Warburg impedance features in the low-frequency domain with straight lines without semicircles,[46] suggesting that the property of the polymer owing to the high electrical resistance and poor conductivity for ionic kinetics in the electrolyte may have surpassed the semicircle. Nevertheless, the area of low frequencies in the catalyst B-catalyzed polymer exhibited a smaller domain than the catalyst A-catalyzed polymer. Although the slope of low frequencies in polymers holding *S. oneidensis* MR-1 as a charge carrier in the electrolyte could significantly

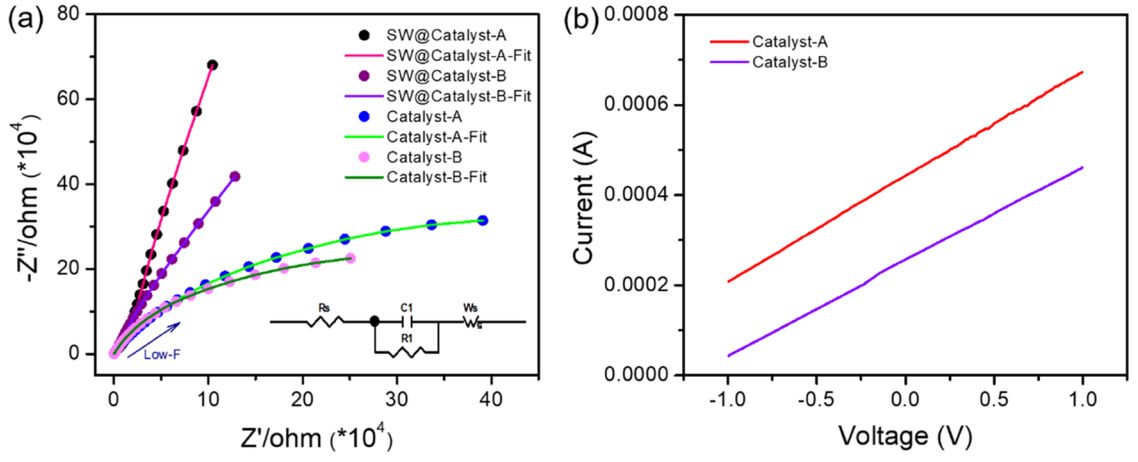

Figure 10. (a) Nyquist plots of EIS spectra from catalyst A- and catalyst B-catalyzed polymers in the electrolytes without a charge carrier using phosphate-buffered saline (PBS) and with a negative charge carrier using exoelectrogenic *S. oneidensis* MR-1 (The blue arrow shows the low-frequency domain on EIS Nyquist plots). (b) Obtained linear curves from polymers as a function of voltage directly proportional to current in terms of ohmic resistance values.

https://doi.org/10.1021/acsomega.2c04123
ACS Omega 2022, 7, 31509−31519

Scheme 2. Electrochemical Workstation with the Polymer (E/1H/VCH) Working Electrode

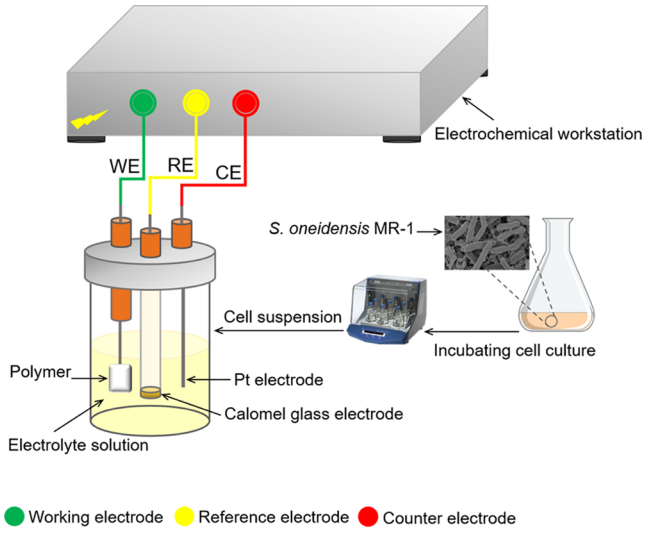

reduce the Warburg resistance, it still could not improve the conductivity, which demonstrated that the external charge supply could not alter the insulating property in the used polymers. As a result, the obtained linear curves between voltage and current in two polymers could determine high ohmic resistance values of 4.28 and 4.77 kΩ for catalyst A and catalyst B, respectively (Figure 10b). The findings indicated that the polymers owing to their distinct insulating properties have poor electrical conductivity.

3.5. Mechanical Properties of the E/1H/VCH Terpolymer. The mechanical properties of the E/1-H/VCH terpolymer produced with catalyst A and catalyst B were calculated at room temperature using an Instron universal testing machine (model 5566, Norwood, MA). The ability to resist external forces in the polymer is mainly due to the chemical bonding of the main chain, interchange interaction, and length of the chain. Therefore, it is reasonable to improve polymer polarity, chain nitration, and chain length to increase its mechanical properties.[46] The effect of 1-hexene and VCH contents in E/1-H/VCH on tensile properties has been analyzed. The stress−strain curves of E/1-H/VCH and fracture are shown in Figure 11.

It reveals that the E/1-H/VCH sample produced with catalyst A shows a higher strength than that of catalyst B because catalyst A produced the E/1-H/VCH polymer with a higher content of 1-hexene (19.06 mol %) and VCH (0.77 mol %) with enhancement in the tensile strength of the polymer, which can be described by increasing length of the chain structure, which was confirmed by the characterization of high-temperature GPC and ^{1}H NMR. Higher insertion of 1-hexene and VCH increases the polymer chain length, and when an external force is applied, more energy is required to fracture the catalyst A-catalyzed E/1-H/VCH polymer. On the other hand, compared with EPDM, due to the higher insertion of propylene, it showed higher energy fracture than the E/1-H/VCH polymer.[47] Thermally stable E/1-hexene/VCH with a higher content of 1-hexene (10−20%) has been prepared with good tensile properties that can be used in the communication, construction, automotive, aerospace, and synthetic rubber industries. In conclusion, the results indicated that the newly synthesized E/1H/VCH terpolymers with both catalysts showed moderate flexural strengths.

4. CONCLUSIONS

In this work, a symmetrical metallocene catalyst system was used to produce a new type of E/1-hexene/VCH-based elastomer with excellent insulating properties. Catalyst A produced the polymer with higher 1-hexene and VCH contents and high

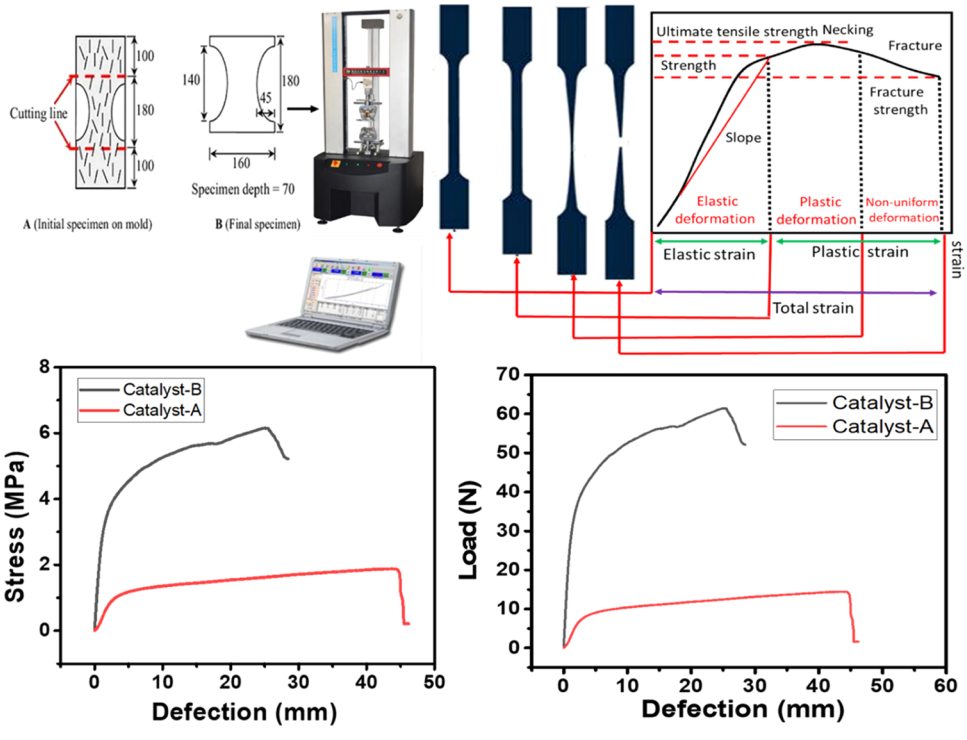

Figure 11. Mechanical properties of the E/1H/VCH terpolymer produced with catalyst A and catalyst B.

https://doi.org/10.1021/acsomega.2c04123
ACS Omega 2022, 7, 31509−31519

molecular weight, while catalyst B showed a higher activity of 1.49×10^6 gm/mmol$_{Mt}$·h and crystalline (ΔH_m of 43.19 J/g) properties. Both catalysts inserted the VCH through exocyclic π bonds, which was confirmed by ^{1}H NMR. In addition, numerous spectroscopic techniques such as ^{1}H NMR, XRD, DSC, GPC, and SEM were used to investigate the microstructure and behavior of the polymers. Second, EIS was used to investigate the polymer interfacial electron transfer properties. The Warburg impedance features in the low-frequency domain with straight lines without semicircles, suggesting the property of the polymer owing to the high electrical resistance. The slope of low frequencies in polymers holding *S. oneidensis* MR-1 as a charge carrier in the electrolyte could significantly reduce the Warburg resistance, which demonstrated that the external charge supply could not alter the insulating property in the E/1-hexene/VCH polymers. These polymers also present a high dielectric constant (k = 6−4) and mechanical properties. Low dielectric loss suggests the suitable application potential of these polymeric materials for the fabrications of capacitors.

AUTHOR INFORMATION

Corresponding Authors

Ahmad Naveed − *Research School of Polymeric Materials, School of Materials Science & Engineering, Jiangsu University, Zhenjiang 212013, P. R. China*; Email: ahmadnaveed@ujs.edu.cn

Li Guo − *Research School of Polymeric Materials, School of Materials Science & Engineering, Jiangsu University, Zhenjiang 212013, P. R. China*; Email: liguo@ujs.edu.cn

Authors

Amjad Ali − *Research School of Polymeric Materials, School of Materials Science & Engineering, Jiangsu University, Zhenjiang 212013, P. R. China; MOE Key Laboratory of Macromolecular Synthesis and Functionalization, Department of Polymer Science and Engineering, Zhejiang University, Hangzhou 310027, P. R. China;* orcid.org/0000-0001-7112-4922

Khulood Fahad Saud Alabbosh − *Department of Biology, College of Science, University of Hail, Hail 81451, Saudi Arabia*

Azim Uddin − *Institute for Composites Science Innovation (InCSI), School of Materials Science and Engineering, Zhejiang University, Hangzhou 310027, P. R. China*

Yanlin Chen − *Institute for Composites Science Innovation (InCSI), School of Materials Science and Engineering, Zhejiang University, Hangzhou 310027, P. R. China*

Tariq Aziz − *School of Engineering Yunqi Campus, Westlake University, Hangzhou, Zhejiang 310024, P. R. China;* orcid.org/0000-0001-8023-9561

Jamile Mohammadi Moradian − *Biofuels Institute, School of Environment, Jiangsu University, Zhenjiang 212013, P. R. China*

Muhammad Imran − *Department of Chemistry, Government College University, Lahore 54000, Pakistan*

Lu Yin − *Research School of Polymeric Materials, School of Materials Science & Engineering, Jiangsu University, Zhenjiang 212013, P. R. China*

Mobashar Hassan − *Research School of Polymeric Materials, School of Materials Science & Engineering, Jiangsu University, Zhenjiang 212013, P. R. China*

Waqar Ahamad Qureshi − *Research School of Polymeric Materials, School of Materials Science & Engineering, Jiangsu University, Zhenjiang 212013, P. R. China*

Muhammad Wajid Ullah − *Biofuels Institute, School of Environment, Jiangsu University, Zhenjiang 212013, P. R. China*

Zhiqiang Fan − *MOE Key Laboratory of Macromolecular Synthesis and Functionalization, Department of Polymer Science and Engineering, Zhejiang University, Hangzhou 310027, P. R. China;* orcid.org/0000-0001-8565-5919

Complete contact information is available at: https://pubs.acs.org/10.1021/acsomega.2c04123

Author Contributions

The article was written through the contributions of all authors. All authors have given approval to the final version of the article.

Notes

The authors declare no competing financial interest.

ACKNOWLEDGMENTS

The authors are thankful to the National Natural Foundation of China (51803081) for their financial support.

REFERENCES

(1) Canaud, C.; Visconte, L. L. Y.; Sens, M. A.; Nunes, R. C. R. Dielectric properties of flame resistant EPDM composites. *Polym. Degrad. Stab.* **2000**, *70*, 259−262.

(2) Zirnstein, B.; Schulze, D.; Schartel, B. The impact of polyaniline in phosphorus flame retardant ethylene-propylene-diene-rubber (EPDM). *Thermochim. Acta* **2019**, *673*, 92−104.

(3) Hlatky, G. G. Metallocene catalysts for olefin polymerization: Annual review for 1996. *Coord. Chem. Rev.* **1999**, *181*, 243−296.

(4) Pittman, C. U. The discovery of metallocene-and metallocene-like addition polymers. *J. Inorg. Organomet. Polym. Mater.* **2005**, *15*, 33−55.

(5) Tritto, I.; Boggioni, L.; Ferro, D. R. Metallocene catalyzed ethene- and propene co-norbornene polymerization: Mechanisms from a detailed microstructural analysis. *Coord. Chem. Rev.* **2006**, *250*, 212−241.

(6) Wong, G. W.; Landis, C. R. Iterative asymmetric hydroformylation/Wittig olefination sequence. *Angew. Chem., Int. Ed.* **2013**, *52*, 1564−1567.

(7) Klosin, J.; Landis, C. R. Ligands for practical rhodium-catalyzed asymmetric hydroformylation. *Acc. Chem. Res.* **2007**, *40*, 1251−1259.

(8) Liu, Z.; Somsook, E.; White, C. B.; Rosaaen, K. A.; Landis, C. R. Kinetics of initiation, propagation, and termination for the [rac-(C2H4 (1-indenyl) 2) ZrMe][MeB (C6F5) 3]-catalyzed polymerization of 1-hexene. *J. Am. Chem. Soc.* **2001**, *123*, 11193−11207.

(9) Liu, Z.; Somsook, E.; Landis, C. R. A 2H-labeling scheme for active-site counts in metallocene-catalyzed alkene polymerization. *J. Am. Chem. Soc.* **2001**, *123*, 2915−2916.

(10) Landis, C. R.; Christianson, M. D. Metallocene-catalyzed alkene polymerization and the observation of Zr-allyls. *Proc. Natl. Acad. Sci. U.S.A.* **2006**, *103*, 15349−15354.

(11) Zanchin, G.; Leone, G. Polyolefin thermoplastic elastomers from polymerization catalysis: Advantages, pitfalls and future challenges. *Prog. Polym. Sci.* **2021**, *113*, No. 101342.

(12) Ali, A.; Liu, X.; Guo, Y.; Akram, M. A.; Wu, H.; Liu, W.; Khan, A.; Jiang, B.; Fu, Z.; Fan, Z. Kinetics and mechanism of ethylene and propylene polymerizations catalyzed with ansa-zirconocene activated by borate/TIBA. *J. Organomet. Chem.* **2020**, *922*, No. 121366.

(13) Ali, A.; Tufail, M. K.; Jamil, M. I.; Yaseen, W.; Iqbal, N.; Hussain, M.; Ali, A.; Aziz, T.; Fan, Z.; Guo, L. Comparative Analysis of Ethylene/Diene Copolymerization and Ethylene/Propylene/Diene Terpolymerization Using Ansa-Zirconocene Catalyst with Alkylaluminum/Borate Activator: The Effect of Conjugated and Nonconjugated Dienes on

Catalytic Behavior and Polymer Microstructure. *Molecules* **2021**, *26*, No. 2037.
(14) Ali, A.; Akram, M. A.; Guo, Y.; Wu, H.; Liu, W.; Khan, A.; Liu, X.; Fu, Z.; Fan, Z. Ethylene−propylene copolymerization and their terpolymerization with dienes using ansa-Zirconocene catalysts activated by borate/alkylaluminum. *J. Macromol. Sci., Part A* **2020**, *57*, 156−164.
(15) Ali, A.; Naveed, A.; Rasheed, T.; Aziz, T.; Imran, M.; Zhang, Z.-K.; Ullah, M. W.; Kubar, A. A.; Rehman, A. U.; Fan, Z.; Guo, L. Methods for Predicting Ethylene/Cyclic Olefin Copolymerization Rates Promoted by Single-Site Metallocene: Kinetics Is the Key. *Polymers* **2022**, *14*, No. 459.
(16) Ali, A.; Muhammad, N.; Hussain, S.; Jamil, M. I.; Uddin, A.; Aziz, T.; Tufail, M. K.; Guo, Y.; Wei, T.; Rasool, G.; et al. Kinetic and thermal study of ethylene and propylene homo polymerization catalyzed by ansa-zirconocene activated with alkylaluminum/borate: Effects of alkylaluminum on polymerization kinetics and polymer structure. *Polymers* **2021**, *13*, No. 268.
(17) Lima, P.; Oliveira, J.; Costa, V. Partial replacement of EPDM by GTR in thermoplastic elastomers based on PP/EPDM: effects on morphology and mechanical properties. *J. Appl. Polym. Sci.* **2014**, *131*, No. 40160.
(18) Tan, J.; Chao, Y.; Wang, H.; Gong, J.; Van Zee, J. Chemical and mechanical stability of EPDM in a PEM fuel cell environment. *Polym. Degrad. Stab.* **2009**, *94*, 2072−2078.
(19) Natali, M.; Rallini, M.; Kenny, J.; Torre, L. Effect of Wollastonite on the ablation resistance of EPDM based elastomeric heat shielding materials for solid rocket motors. *Polym. Degrad. Stab.* **2016**, *130*, 47−57.
(20) Prabu, R. R.; Usa, S.; Udayakumar, K.; Khan, M. A.; Majeed, S. A. Electrical insulation characteristics of silicone and epdm polymeric blends. I. *IEEE Trans. Dielectr. Electr. Insul.* **2007**, *14*, 1207−1214.
(21) Hamzah, M. S.; Jaafar, M.; Mohd Jamil, M. K. Electrical insulation characteristics of alumina, titania, and organoclay nanoparticles filled PP/EPDM nanocomposites. *J. Appl. Polym. Sci.* **2014**, *131*, No. 41184.
(22) Ehsani, M.; Borsi, H.; Gockenbach, E.; Bakhsahnde, G.; Morshedian, J.; Abedi, N. In *Study of Electrical, Dynamic Mechanical and Surface Properties of Silicone-EPDM Blends*, Proceedings of the 2004 IEEE International Conference on Solid Dielectrics; IEEE, 2004; pp 431−434.
(23) Chi, Q. G.; Yang, M.; Zhang, C.; Zhang, T.; Feng, Y.; Chen, Q. Nonlinear electrical conductivity and thermal properties of AgNPs/BN/EPDM composites for cable accessory. *IEEE Trans. Dielectr. Electr. Insul.* **2019**, *26*, 1081−1088.
(24) Niu, X.; Stoyanov, H.; Hu, W.; Leo, R.; Brochu, P.; Pei, Q. Synthesizing a new dielectric elastomer exhibiting large actuation strain and suppressed electromechanical instability without prestretching. *J. Polym. Sci., Part B: Polym. Phys.* **2013**, *51*, 197−206.
(25) Gu, K.; Loo, Y. L. The polymer physics of multiscale charge transport in conjugated systems. *J. Polym. Sci., Part B: Polym. Phys.* **2019**, *57*, 1559−1571.
(26) Wang, B. Ansa-metallocene polymerization catalysts: Effects of the bridges on the catalytic activities. *Coord. Chem. Rev.* **2006**, *250*, 242−258.
(27) Ali, A.; Nadeem, M.; Lu, J.; Moradian, J. M.; Rasheed, T.; Aziz, T.; Maouche, C.; Guo, Y.; Awais, M.; Zhiqiang, F.; Quo, L. Rapid kinetic evaluation of homogeneous single-site metallocene catalysts and cyclic diene: how do the catalytic activity, molecular weight, and diene incorporation rate of olefins affect each other? *RSC Adv.* **2021**, *11*, 31817−31826.
(28) Ali, A.; Jamil, M. I.; Uddin, A.; Hussain, M.; Aziz, T.; Tufail, M. K.; Guo, Y.; Jiang, B.; Fan, Z.; Guo, L. Kinetic and thermal study of ethylene-propylene copolymerization catalyzed by ansa-zirconocene activated with Alkylaluminium/borate: Effects of linear and branched alkylaluminium compounds as cocatalyst. *J. Polym. Res.* **2021**, *28*, 1−15.
(29) Jamil, M. I.; Wang, Q.; Ali, A.; Hussain, M.; Aziz, T.; Zhan, X.; Zhang, Q. Slippery Photothermal Trap for Outstanding Deicing Surfaces. *J. Bionic Eng.* **2021**, *18*, 548−558.
(30) Ali, A.; Uddin, A.; Jamil, M. I.; Shen, X.; Abbas, M.; Aziz, T.; Hussain, M.; Hussain, S.; Fang, R.; Fan, Z.; Guo, L. Kinetics and mechanistic investigations of ethylene-propylene copolymerizations catalyzed with symmetrical metallocene and activated by TIBA/borate. *J. Organomet. Chem.* **2021**, *949*, No. 121929.
(31) Yang, Y.; Yu, Y.-Y.; Shi, Y.-T.; Moradian, J. M.; Yong, Y.-C. In Vivo Two-Way Redox Cycling System for Independent Duplexed Electrochemical Signal Amplification. *Anal. Chem.* **2019**, *91*, 4939−4942.
(32) Cheng, L.; Min, D.; He, R. L.; Cheng, Z. H.; Liu, D. F.; Yu, H. Q. Developing a base-editing system to expand the carbon source utilization spectra of *Shewanella oneidensis* MR-1 for enhanced pollutant degradation. *Biotechnol. Bioeng.* **2020**, *117*, 2389−2400.
(33) Yong, Y.-C.; Dong, X.-C.; Chan-Park, M. B.; Song, H.; Chen, P. Macroporous and monolithic anode based on polyaniline hybridized three-dimensional graphene for high-performance microbial fuel cells. *ACS Nano* **2012**, *6*, 2394−2400.
(34) Ali, A.; Akram, M. A.; Guo, Y.; Wu, H.; Liu, W.; Khan, A.; Liu, X.; Fu, Z.; Fan, Z. Ethylene−propylene copolymerization and their terpolymerization with dienes using *ansa*-Zirconocene catalysts activated by borate/alkylaluminum. *Journal of Macromolecular Science, Part A* **2020**, *57* (2), 156−164.
(35) Chu, K. J.; Shan, C. L. P.; Soares, J. B.; Penlidis, A. Copolymerization of ethylene and 1-hexene with in-situ supported Et [Ind] 2ZrCl2. *Macromol. Chem. Phys.* **1999**, *200*, 2372−2376.
(36) Boggioni, L.; Sidari, D.; Losio, S.; Stehling, U. M.; Auriemma, F.; Di Girolamo, R.; De Rosa, C.; Tritto, I. Ethylene−co−norbornene copolymerization in the presence of a chain transfer agent. *Eur. Polym. J.* **2018**, *107*, 54−66.
(37) Malmberg, A.; Kokko, E.; Lehmus, P.; Löfgren, B.; Seppälä, J. V. Long-chain branched polyethene polymerized by metallocene catalysts Et [Ind] 2ZrCl2/MAO and Et [IndH4] 2ZrCl2/MAO. *Macromolecules* **1998**, *31*, 8448−8454.
(38) Malmberg, A.; Löfgren, B. The production of ethene/propene/5-ethylidene-2-norbornene terpolymers using metallocene catalysts: Polymerization, characterization and properties of the metallocene EPDM. *J. Appl. Polym. Sci.* **1997**, *66*, 35−44.
(39) Ali, A.; Naveed, A.; Shehzad, K.; Aziz, T.; Rasheed, T.; Moradian, J. M.; Hassan, M.; Rahman, A.; Zhiqiang, F.; Guo, L. Polymerization kinetics of bicyclic olefins and mechanism with symmetrical ansa-metallocene catalysts associated with active center count: relationship between their activities and structure and activation path. *RSC Adv.* **2022**, *12*, 15284−15295.
(40) Mortazavi, M.; Arabi, H.; Ahmadjo, S.; Nekoomanesh, M.; Zohuri, G. Comparative study of copolymerization and terpolymerization of ethylene/propylene/diene monomers using metallocene catalyst. *J. Appl. Polym. Sci.* **2011**, *122*, 1838−1846.
(41) Jiang, B.; Zhang, B.; Guo, Y.; Ali, A.; Guo, W.; Fu, Z.; Fan, Z. Effects of titanium dispersion state on distribution and reactivity of active centers in propylene polymerization with MgCl2-supported Ziegler-Natta catalysts: A kinetic study based on active center counting. *ChemCatChem* **2020**, *12*, 5140−5148.
(42) Chi, Q.; Yang, M.; Zhang, T.; Zhang, C. Investigation of electrical and mechanical properties of silver-hexagonal boron nitride/EPDM composites. *J. Mater. Sci.: Mater. Electron.* **2019**, *30*, 13321−13329.
(43) Zhang, K.; Yu, X. Catalyst-free and low-temperature terpolymerization in a single-component benzoxazine resin containing both norbornene and acetylene functionalities. *Macromolecules* **2018**, *51*, 6524−6533.
(44) Zhang, K.; Yu, X.; Kuo, S.-W. Outstanding dielectric and thermal properties of main chain-type poly (benzoxazine-co-imide-co-siloxane)-based cross-linked networks. *Polym. Chem.* **2019**, *10*, 2387−2396.
(45) Prasad Sahoo, B.; Naskar, K.; Kumar Tripathy, D. Multiwalled carbon nanotube-filled ethylene acrylic elastomer nanocomposites: influence of ionic liquids on the mechanical, dynamic mechanical, and dielectric properties. *Polym. Compos.* **2016**, *37*, 2568−2580.
(46) Barbero, G. Warburg's impedance revisited. *Phys. Chem. Chem. Phys.* **2016**, *18*, 29537−29542.

https://doi.org/10.1021/acsomega.2c04123
ACS Omega 2022, 7, 31509−31519

(47) Xiong, C.; Li, X.; He, H.; Xue, B.; Wang, Y.; Li, J.; Zhu, Z. A thermally reversible healing EPDM based elastomer with higher tensile properties and damping properties. *J. Appl. Polym. Sci.* **2021**, *138*, No. 49767.

https://doi.org/10.1021/acsomega.2c04123
ACS Omega 2022, 7, 31509−31519